Mass parameters in the adiabatic time-dependent Hartree-Fock approximation. II. Results for the isoscalar quadrupole mode

M. J. Giannoni and P. Quentin*
Division de Physique Théorique, Institut de Physique Nucléaire, 91406 Orsay-Cedex, France
(Received 2 August 1979)

The formalism presented in the preceding paper is used to compute self-consistent adiabatic mass parameters for the isoscalar quadrupole modes. Skyrme-like effective forces have been used. A detailed study of the practical methods of calculation is made. A special attention is devoted to the problem of numerical accuracy. Results are presented for both scaling and constrained Hartree-Fock paths. A comparative discussion of the two corresponding sets of results is made. The method used to calculate self-consistent mass parameters for the constrained Hartree-Fock path provides, as a byproduct, the non-self-consistent cranking mass. This method (for self-consistent as well as cranking masses) is free of continuum problems inherent to the application of the usual cranking formula. The effect of self-consistency is extensively studied by use of a large set of Skyrme-like forces.

NUCLEAR STRUCTURE ^{12}C, ^{16}O, ^{40}Ca, ^{48}Ca, ^{56}Ni, ^{90}Zr, ^{140}Ce, ^{208}Pb; mass parameters for isoscalar quadrupole collective motion calculated within time-dependent Hartree-Fock approximation in adiabatic limit. Skyrme-like forces used. Numerical accuracy discussed. Self-consistent results for both scaling and constrained Hartree-Fock paths discussed. Validity of Inglis cranking masses assessed. Influence of forces studied.

I. INTRODUCTION

In an accompanying paper,[1] hereafter referred to as I, a theoretical study of the adiabatic time-dependent Hartree-Fock (ATDHF) approximation was presented, where attention was focused on the particular case of a collective path parametrized by a single collective variable. The ATDHF formalism allows then the calculation of the corresponding mass parameter through the solution of the first set of Hamilton-like equations of motion.

Two choices for the parametrization of the path were discussed in detail. In the first choice, the trajectory is given by the solution of a constrained Hartree-Fock (CHF) problem, i.e., is fixed by the guess of a constraining operator. In the second choice, the path is obtained by scaling a static Hartree-Fock wave function. In this second case, the computation of the mass is straightforward. In the former case we have shown that the inversion of the first set of Hamilton equations providing the mass parameter can be advantageously replaced by the solution of a double CHF problem.

The content of paper I was rather general. No particular form was assumed for the effective nucleon-nucleon interaction and, except for the illustration of some specific points, no explicit mention was made of particular excitation modes. In the present paper, we apply the formalism of I to the study of isoscalar quadrupole Q_{20} vibrations. As effective interactions, we shall use Skyrme forces, which have been quite successful for the description of many static nuclear properties.[2-6]

In Sec. II we summarize the method of the calculation, and give some of the necessary formulas for the case where Skyrme forces are used and some symmetries assumed for the ATDHF solutions. Section III is devoted to the discussion of several numerical problems, including the convergence of the mass parameters with respect to the size of the truncated basis on which we expand the CHF orbitals. The results of our calculations are presented, and their physical significance discussed in Sec. IV.

II. CALCULATION OF QUADRUPOLE ADIABATIC MASSES WITH SKYRME-LIKE FORCES

A. General outline of the calculations

For the two choices of the path we have considered, we present the practical method of calculation of the mass parameter.

The quadrupole scaling path. In this case, we perform a static Hartree-Fock (HF) calculation, providing an equilibrium one-body reduced density operator ρ_{st}. The corresponding radius and quadrupole moment are called r_{st} and q_{st}. If the effective interaction is gauge invariant with respect to the isoscalar excitation operator Q_{20} (we will see in Sec. II B that it is so for the Skyrme forces in use in this work), the scaling mass

parameter is given as a function of the quadrupole moment $q=\langle Q_{20}\rangle$ by

$$M_{\mathrm{SC}}(q)=\frac{m}{8Ar^2+4q}, \tag{2.1}$$

where r is deduced from q through the following equations up to first order in the scaling parameter β:

$$Ar^2=\frac{(1-2\beta)^2}{3}(2Ar_{\mathrm{st}}{}^2-q_{\mathrm{st}}) + \frac{1}{3(1-2\beta)^4}(Ar_{\mathrm{st}}{}^2+q_{\mathrm{st}}), \tag{2.2}$$

$$q=\frac{(1-2\beta)^2}{3}(q_{\mathrm{st}}-2Ar_{\mathrm{st}}{}^2) + \frac{2}{3(1-2\beta)^4}(Ar_{\mathrm{st}}{}^2+q_{\mathrm{st}}). \tag{2.3}$$

The CHF path with the external field Q_{20}. The calculations are performed in two steps. We first get the adiabatic path $\rho_0(q)$ from a CHF calculation for the time-even constraining field $(-\lambda Q_{20})$

$$[W_0-\lambda Q_{20},\rho_0]=0, \tag{2.4}$$

where W_0 is the Hartree-Fock Hamiltonian built from ρ_0. The path $\rho_0(q)$ is parametrized by the variable $q=\mathrm{Tr}Q_{20}\rho_0$ corresponding to the Lagrange multiplier λ.

When this is achieved, one can compute numerically the matrix $\partial\rho_0/\partial q$, and therefore calculate the "momentum" operator P generating the dynamics [see in I Eq. (4.5) and the related discussion). This time-odd operator enters in the double CHF equation, equivalent to the first ATDHF equation [see Eq. (2.24) of I]:

$$[W_0+W_1-\lambda Q_{20}^A-\dot{q}P,\rho_0+\rho_1]=0, \tag{2.5}$$

where Q_{20}^A is the antidiagonal part of Q_{20} $[Q_{20}^A=\rho_0Q_{20}(1-\rho_0)+(1-\rho_0)Q_{20}\rho_0]$, and where the velocity parameter $\dot{q}$ must be chosen small enough to ensure the linear response.

This CHF equation is solved iteratively by taking as a first guess for the solution the time-even density ρ_0 obtained by solving Eq. (2.4) with the same value of the Lagrange multiplier λ. At the first iteration, we get a time-odd density $\rho_1{}^1$ which is the non-self-consistent response of the system to the time-odd perturbating field $(-\dot{q}P)$; this $\rho_1{}^1$ is therefore calculated in the *Inglis cranking* approximation.

Once ρ_1 is determined, the mass parameter is given by

$$M(q)=\mathrm{Tr}(P\rho_1)/\dot{q}. \tag{2.6}$$

This formula is of course valid for a self-consistent as well as for a non-self consistent (Inglis cranking) operator ρ_1.

B. The effective forces

As for phenomenological effective forces we use Skyrme-like forces which, in the $\vec{r}$ representation, write

$$V_{\mathrm{sk}}(\vec{r}_1,\vec{r}_2)=t_0(1+x_0\mathcal{P}_\sigma)\delta(\vec{r})+\tfrac{1}{2}t_1(1+x_1\mathcal{P}_\sigma)\{\vec{P}'{}^2\delta(\vec{r})+\delta(\vec{r})\vec{P}^2\} + t_2(1+x_2\mathcal{P}_\sigma)\vec{P}'\cdot\delta(\vec{r})\vec{P}+iw_0\vec{\sigma}\cdot\{\vec{P}'\times\delta(\vec{r})\vec{P}\}+\tfrac{1}{6}t_3(1+x_3\mathcal{P}_\sigma)\{\rho(\vec{R})\}^\alpha\delta(\vec{r}) \tag{2.7}$$

with

$\vec{r}=\vec{r}_1-\vec{r}_2$,

$\vec{R}=(\vec{r}_1+\vec{r}_2)/2$,

$\vec{P}=(\vec{\nabla}_1-\vec{\nabla}_2)/2i$ ($\vec{P}'$ being the complex conjugate of $\vec{P}$ acting on its left-hand side)

$\vec{\sigma}=\vec{\sigma}_1+\vec{\sigma}_2$ ($\vec{\sigma}_i$ being a Pauli spin matrix acting in the i subspace)

$\mathcal{P}_\sigma=(1+\vec{\sigma}_1\cdot\vec{\sigma}_2)/2$.

Notice that, due to the presence in $V_{\mathrm{sk}}(\vec{r}_1,\vec{r}_2)$ of $\delta(\vec{r}_1-\vec{r}_2)$, there is no need to introduce other exchange operators than $\mathcal{P}_\sigma$.

These forces depend on 10 parameters. Most of the time we consider in this work forces such that $x_1=x_2=0$ and $x_3=\alpha=1$. For this class of forces an extensive study of the parameter adjustment has been done in Ref. 5. It has been found that imposing only a good reproduction of nuclear matter (or equivalently magic nuclei) saturation properties is not sufficient for a complete determination of the parameter set. The remaining freedom is associated with the well known fact that nuclear matter saturation can be obtained either by a velocity-dependent interaction, or by a density-dependent interaction, or by a mixture of these two types of forces. One may thus characterize saturating Skyrme forces by their effective mass m^* in nuclear matter, i.e., by their velocity dependence. By adjusting the parameters to static properties of nonmagic nuclei, one obtains a small range of acceptable values for m^*. The SIII force, for which m^*

$=0.76$ (in units of the nucleonic mass m), gives a particularly good fit to a large number of experimental data.[6]

For a Slater determinant $|\psi\rangle$ the expectation value of the Hamiltonian H:

$$H = T + V_{\text{sk}} + V_{\text{coul}}, \tag{2.8}$$

where T is the kinetic energy operator and V_{coul} the Coulomb interaction, can be written as the integral of a Hamiltonian density

$$\langle\psi|H|\psi\rangle = \int \mathcal{H}(\vec{r})d^3r. \tag{2.9}$$

The Hamiltonian density $\mathcal{H}$ is defined by[7,8]

$$\begin{aligned}
\mathcal{H}(\vec{r}) = {} & \frac{\hbar^2}{2m}\tau + \tfrac{1}{2}t_0\Big((1+\tfrac{1}{2}x_0)\rho^2 - (x_0+\tfrac{1}{2})\sum_q(\rho^q)^2 + \tfrac{1}{2}x_0\vec{\rho}^2 - \tfrac{1}{2}\sum_q(\vec{\rho}^q)^2\Big) \\
& + \tfrac{1}{4}t_1\Big((1+\tfrac{1}{2}x_1)[\rho\tau - \vec{j}^2 + \tfrac{3}{4}(\vec{\nabla}\rho)^2] - (x_1+\tfrac{1}{2})\sum_q[\rho^q\tau^q - (\vec{j}^q)^2 + \tfrac{3}{4}(\vec{\nabla}\rho^q)^2] \\
& \quad + \tfrac{1}{2}x_1[\vec{\rho}\cdot\vec{\tau} - ((J_{\mu\nu}))^2 + \tfrac{3}{4}((\nabla_\mu\rho_\nu))^2] - \tfrac{1}{2}\sum_q[\vec{\rho}^q\cdot\vec{\tau}^q - ((J^q_{\mu\nu}))^2 + \tfrac{3}{4}((\nabla_\mu\rho^q_\nu))^2]\Big) \\
& + \tfrac{1}{4}t_2\Big((1+\tfrac{1}{2}x_2)[\rho\tau - \vec{j}^2 - \tfrac{1}{4}(\vec{\nabla}\rho)^2] + (x_2+\tfrac{1}{2})\sum_q[\rho^q\tau^q - (\vec{j}^q)^2 - \tfrac{1}{4}(\vec{\nabla}\rho^q)^2] \\
& \quad + \tfrac{1}{2}x_2[\vec{\rho}\cdot\vec{\tau} - ((J_{\mu\nu}))^2 - \tfrac{1}{4}((\nabla_\mu\rho_\nu))^2] + \tfrac{1}{2}\sum_q[\vec{\rho}^q\cdot\vec{\tau}^q - ((J^q_{\mu\nu}))^2 - \tfrac{1}{4}((\nabla_\mu\rho^q_\nu))^2]\Big) \\
& + \tfrac{1}{12}t_3\rho^\alpha\Big((1+\tfrac{1}{2}x_3)\rho^2 - \sum_q[(x_3+\tfrac{1}{2})(\rho^q)^2] + \tfrac{1}{2}x_3\vec{\rho}^2 - \tfrac{1}{2}\sum_q(\vec{\rho}^q)^2\Big) \\
& - \frac{w_0}{2}\Big(i\sqrt{2}[\vec{J}\cdot\vec{\nabla}\rho + \sum_q(\vec{J}^q\cdot\vec{\nabla}\rho^q)] + \vec{\nabla}\times\vec{\rho}\cdot\vec{j} + \sum_q(\vec{\nabla}\times\vec{\rho}^q\cdot\vec{j}^q)\Big) + \mathcal{H}_{\text{coul}}.
\end{aligned} \tag{2.10}$$

The six density functions[9] appearing in Eq. (2.10) are defined in terms of the one-body density matrix ρ,

$$\rho(\vec{r},\sigma;\vec{r}',\sigma') = \sum_i \psi_i^*(\vec{r}',\sigma')\psi_i(\vec{r},\sigma), \tag{2.11}$$

(where the ψ_i's are occupied orbitals) by

$$\begin{aligned}
\rho(\vec{r}) &= \sum_\sigma \rho(\vec{r},\sigma;\vec{r},\sigma), \\
\vec{\rho}(\vec{r}) &= \sum_{\sigma,\sigma'}\rho(\vec{r},\sigma;\vec{r},\sigma')\langle\sigma'|\vec{\sigma}|\sigma\rangle, \\
\tau(\vec{r}) &= \sum_\sigma \vec{\nabla}\cdot\vec{\nabla}'\rho(\vec{r},\sigma;\vec{r}',\sigma)]_{\vec{r}'=\vec{r}}, \\
\vec{\tau}(\vec{r}) &= \sum_{\sigma,\sigma'}\vec{\nabla}\cdot\vec{\nabla}'\rho(\vec{r},\sigma;\vec{r}',\sigma')]_{\vec{r}'=\vec{r}}\langle\sigma'|\vec{\sigma}|\sigma\rangle, \\
\vec{j}(\vec{r}) &= \frac{1}{2i}\sum_\sigma(\vec{\nabla}-\vec{\nabla}')\rho(\vec{r},\sigma;\vec{r}',\sigma)]_{\vec{r}'=\vec{r}}, \\
J_{\mu\nu}(\vec{r}) &= \frac{1}{2i}\sum_{\sigma,\sigma'}(\nabla_\mu - \nabla'_\mu)\rho(\vec{r},\sigma;\vec{r}',\sigma')]_{\vec{r}'=\vec{r}} \\
&\quad \times\langle\sigma'|\sigma_\nu|\sigma\rangle,
\end{aligned} \tag{2.12}$$

where the indices μ,ν label the spherical components of the vectors $\vec{\rho}$, $\vec{\nabla}$ and $\vec{\sigma}$. The Hamiltonian density (2.10) involves two tensorial products,

$$\begin{aligned}
((J_{\mu\nu}))^2 &= \sum_{\mu\nu}(-)^{\mu+\nu}J_{\mu\nu}J_{-\mu-\nu} \\
&= (J^{(0)})^2 - (J^{(1)})^2 + (J^{(2)})^2
\end{aligned} \tag{2.13}$$

and

$$\begin{aligned}
((\nabla_\mu\rho_\nu))^2 &= ([\vec{\nabla}\otimes\vec{\rho}]^{(0)})^2 - ([\vec{\nabla}\otimes\vec{\rho}]^{(1)})^2 \\
&\quad + ([\vec{\nabla}\otimes\vec{\rho}]^{(2)})^2 \\
&= \tfrac{1}{3}(\vec{\nabla}\cdot\vec{\rho})^2 + \tfrac{1}{2}(\vec{\nabla}\times\vec{\rho})^2 \\
&\quad + ([\vec{\nabla}\otimes\vec{\rho}]^{(2)})^2,
\end{aligned} \tag{2.14}$$

where $J^{(i)}$ and $[\vec{\nabla}\otimes\vec{\rho}]^{(i)}$ are the irreducible components of rank i of the tensors J and $\vec{\nabla}\otimes\vec{\rho}$. In Eq. (2.10) the vector component $J^{(1)}$ of J has been noted $\vec{J}$ [it is $i/\sqrt{2}$ times the spin-density $\vec{J}$ of Eq. (11) in Ref. 2]. To be consistent with the phenomenological determination of the force parameters made in Ref. 5 we shall neglect in $\mathcal{H}(\vec{r})$ the contribution of the tensors of rank 1 and 2 to $((J_{\mu\nu}))^2$. The superscript q in Eq. (2.10) indicates the charge state (which cannot be confused with the collective variable q); the total (neutron + proton) densities (2.12) are therefore given by

$$\rho(\vec{r}) = \sum_q \rho^q(\vec{r}) \tag{2.15}$$

and by similar formulas. Finally, the Coulomb energy density is written in terms of the proton density $\rho^p(\vec{r})$ as

$$\mathcal{H}_{\text{coul}}(\vec{r})=\frac{e^2}{2}\rho^p(\vec{r})\left\{\int\frac{\rho^p(\vec{r}')}{|\vec{r}-\vec{r}'|}d^3r'-\frac{3}{2}\left(\frac{3}{\pi}\right)^{1/3}[\rho^p(\vec{r})]^{4/3}\right\}, \quad (2.16)$$

where the last term is a local approximation, due to Gombàs,[10] of the Coulomb exchange contribution.

In relation with the discussion made in I about the scaling path, we notice that the central *and* the spin-orbit parts of the Skyrme force are invariant for isoscalar gauge transformations (see Appendix A). This holds in particular for the description of isoscalar quadrupole modes with Skyrme forces presented in Sec. IV.

C. Symmetries

Let us associate to a particular collective mode, an operator Q which possesses some symmetries. It is reasonable to assume that the ATDHF solution shares the same symmetries. Because the numerical calculations of Sec. IV correspond to the isoscalar operator $Q=Q_{20}$, we shall now assume that ρ has the following symmetries:

(i) the axial symmetries

$$R_3^s(\theta)=e^{i\theta s_3},$$
$$R_3^x(\theta)=e^{i\theta l_3}, \quad (2.17)$$

for both spin and space variables,

(ii) the parity symmetry P_0,

(iii) the reflection symmetry

$$U_2=P_0e^{i\pi(l_2+s_2)} \quad (2.18)$$

with respect to the 1-3 coordinate plane.

Notice that if one defines the operators U_1 and U_3 as in Eq. (2.18), the symmetries (i) and (ii) imply the symmetry under U_3. Since

$$U_1U_2U_3=P_0, \quad (2.19)$$

the symmetries (i), (ii), and (iii) imply the symmetry under U_1. If one assumes that the symmetries (i) and (ii) are satisfied and that ρ is time even (e.g., ρ_0 in our case), one can show (see Appendix B) that ρ commutes also then with U_2, and therefore with U_1.

Let us now investigate the implications of the symmetries (i), (ii), and (iii) on the two step determination of ρ_0 and $\rho_0+\rho_1$. We first prove that the equations

$$[V,R_3^x]=[V,R_3^s]=[V,P_0]=0 \quad (2.20)$$

and

$$[Q_{20},R_3^x]=[Q_{20},R_3^s]=[Q_{20},P_0]=0, \quad (2.21)$$

imply the existence of a solution of the ATDHF equations such that

$$[\rho_0,R_3^x]=[\rho_0,R_3^s]=[\rho_0,P_0]=0 \quad (2.22)$$

and

$$[\rho_1,R_3^x]=[\rho_1,R_3^s]=[\rho_1,P_0]=0. \quad (2.23)$$

Indeed, Eq. (2.22) follows from the symmetry assumptions and from the well known theorem on consistent symmetries (see, e.g., Ref. 11) applied to the Hamiltonian $H-\lambda Q_{20}$. Furthermore, from the definition of the operator P [see Eq. (4.5) of I], we have

$$[P,R_3^x]=[P,R_3^s]=[P,P_0]=0. \quad (2.24)$$

This is because P, being an algebraic function of ρ_0 and $\partial\rho_0/\partial q$, has the same symmetries (2.22). If we now apply the theorem on consistent symmetries to the Hamiltonian $H-\lambda Q_{20}^A-\dot{q}P$ we obtain

$$[\rho,R_3^x]=[\rho,R_3^s]=[\rho,P_0]=0 \quad (2.25)$$

and then Eq. (2.23).

The symmetry properties of ρ greatly simplify the numerical calculations. Indeed, it can be shown (see Appendix C) that Eqs. (2.22) and (2.23) imply

$$\vec{\rho}=\vec{\tau}=J_{\mu\nu}^{(0)}=j_\theta=0, \quad (2.26)$$

where j_θ is the θ component of the current $\vec{j}$ in cylindrical coordinates. The vanishing of $J_{\mu\nu}^{(0)}$, combined with the dropping of $J_{\mu\nu}^{(1)}$ and $J_{\mu\nu}^{(2)}$, suppresses any contribution of $((J_{\mu\nu}))^2$ to $\mathcal{H}$.

As a consequence of Eq. (2.26), the introduction of a time-odd constraint P requires only two new density functions j_r and j_z to those needed in the "ordinary" static CHF calculations of the type discussed in Refs. 3 and 4. This illustrates the considerable simplification brought in by the symmetry requirements.

D. The Hartree-Fock Hamiltonian

The doubly constrained HF equations are obtained by the minimization of the quantity

$$F=\int\mathcal{H}(\vec{r})d^3r-\lambda\langle Q_{20}^A\rangle-\dot{q}\langle P\rangle-\sum_i e_i\int|\psi_i(\vec{r})|^2d^3r \quad (2.27)$$

with respect to the variations of the occupied orbitals ψ_i. The expression (2.27) contains the total energy defined by Eq. (2.10), the energies corresponding to the external fields Q_{20}^A and P, and constraining terms

ensuring the norm conservation of each occupied orbital. Considering only the CHF solutions with the symmetries which have just been discussed, one obtains[7] the following equation for an orbital ψ_j of charge q:

$$\left[-\vec{\nabla}\cdot\frac{\hbar^2}{2m_q^*(\vec{r})}\vec{\nabla}+U^q(\vec{r})-i\vec{W}^q(r)\cdot(\vec{\nabla}\times\vec{\sigma})+\vec{W}_1^q(\vec{r})-e_j\right]\psi_j(\vec{r})+\int U^{\text{ext}}(\vec{r},\vec{r}')\psi_j(\vec{r}')d^3r'=0\,. \tag{2.28}$$

In Eq. (2.28), the effective mass $m_q^*(\vec{r})$ is given by

$$\frac{\hbar^2}{2m_q^*(\vec{r})}=\frac{\hbar^2}{2m}+\tfrac{1}{4}[t_1(1+\tfrac{1}{2}x_1)+t_2(1+\tfrac{1}{2}x_2)]\rho-\tfrac{1}{4}[t_1(\tfrac{1}{2}+x_1)-t_2(\tfrac{1}{2}+x_2)]\rho^q\,, \tag{2.29}$$

the central field $U^q(\vec{r})$ is

$$\begin{aligned}U^q(\vec{r})=&\,t_0[(1+\tfrac{1}{2}x_0)\rho-(x_0+\tfrac{1}{2})\rho^q]+\tfrac{1}{8}[3(1+\tfrac{1}{2}x_1)t_1-(1+\tfrac{1}{2}x_2)t_2]\vec{\nabla}^2\rho\\&+\tfrac{1}{8}[3(\tfrac{1}{2}+x_1)t_1+(\tfrac{1}{2}+x_2)t_2]\vec{\nabla}^2\rho^q+\tfrac{1}{4}[(1+\tfrac{1}{2}x_1)t_1+(1+\tfrac{1}{2}x_2)t_2]\tau\\&-\tfrac{1}{4}[(\tfrac{1}{2}+x_1)t_1-(\tfrac{1}{2}+x_2)t_2]\tau^q+\tfrac{1}{12}t_3\{(1+\tfrac{1}{2}x_3)(2+\alpha)(\rho)^{\alpha+1}-(x_3+\tfrac{1}{2})[\alpha(\rho)^{\alpha+1}(\rho^q)^2+2(\rho)^\alpha\rho^q]\}\\&+\frac{i}{\sqrt{2}}w_0(\vec{\nabla}\cdot\vec{J}+\vec{\nabla}\cdot\vec{J}^q)+\delta_{q,\text{proton}}\tfrac{1}{2}e^2\left\{\int\frac{\rho^q(\vec{r}')}{|\vec{r}-\vec{r}'|}d^3r'-2\left[\frac{3}{\pi}\rho^q(\vec{r})\right]^{1/3}\right\},\end{aligned} \tag{2.30}$$

the spin-orbit field $\vec{W}^q(\vec{r})$ is

$$\vec{W}^q(r)=\tfrac{1}{2}w_0(\vec{\nabla}\rho+\vec{\nabla}\rho^q)\,, \tag{2.31}$$

the time-odd field $W_1^q(\vec{r})$ is

$$W_1^q(\vec{r})=\frac{1}{2i}[\vec{I}^q(\vec{r})\cdot\vec{\nabla}+\vec{\nabla}\cdot\vec{I}^q(\vec{r})] \tag{2.32}$$

with

$$\begin{aligned}\vec{I}^q(\vec{r})=&-\tfrac{1}{2}[t_1(1+\tfrac{1}{2}x_1)+t_2(1+\tfrac{1}{2}x_2)]\vec{j}(\vec{r})\\&+\tfrac{1}{2}[t_1(\tfrac{1}{2}+x_1)-t_2(\tfrac{1}{2}+x_2)]\vec{j}^q(\vec{r})\,,\end{aligned} \tag{2.33}$$

and the external (non local) field $U_{\text{ext}}(\vec{r},\vec{r}')$ is

$$U^{\text{ext}}(\vec{r},\vec{r}')=-\langle\vec{r}|\lambda Q_{20}^A+\dot{q}P|\vec{r}'\rangle\,. \tag{2.34}$$

To solve the set of coupled equations (2.28), we expand each orbital ψ_i on a truncated set of eigenfunctions of the axially symmetric harmonic oscillator. We shall discuss in Sec. III the numerical problems related to this truncation. Notice that these basis states fulfill the symmetry requirements of Sec. II C. The expansion of the ψ_i's converts the solution of Eqs. (2.28) into the diagonalization of a Hermitian complex matrix which is performed by the usual Jacobi method.[12] To construct the Hamiltonian matrix, we perform a numerical integration for the kinetic energy, U^q and $\vec{W}^q$, following the methods of Ref. 3. These methods have been extended to include the time-odd field W_1^q (see Appendix D). For the contribution of the external field U^{ext}, due to its nonlocality, we have computed its matrix elements in the harmonic oscillator basis. This is easy for P since we know how to express ρ_0 and $\partial\rho_0/\partial q$ on this basis. For Q_{20}^A, we need to compute the matrix elements of Q_{20} in the expansion basis which is readily performed according to the methods developed in Ref. 13.

Notice that even though the HF states belonging to a subspace Ω^π (Ω being the third component of the total angular momentum and π the parity) are *not* complex conjugates of the states belonging to the subspace $-\Omega^\pi$, their respective contributions to the different density functions are equal. This is due to the imposed symmetries, as shown in Appendix B, and leads to an important simplification, in the computation of the various terms of Eq. (2.28). It may be also worth recalling that the formalism has been developed in I for two-body density-independent forces; introducing the most general two body density-dependent or three-body forces would result in a more involved expression for the operator W_1. However, the density-dependent part of the Skyrme interaction contributes only to W_0 once the symmetries which we have imposed are properly taken into account. For this reason, the expression (2.22) of paper I for W_1 remains correct for Skyrme-like forces.

III. SOME COMMENTS ON NUMERICAL PROBLEMS

For both choices of the adiabatic path, one has first to solve a static HF equation (with, or without a time-even constraint). In the case of the CHF collective trajectory, one must solve a second CHF equation, with a double (time-even plus time-odd) constraint. This is done, as already indicated in Sec. II D, by expanding the CHF orbitals on a truncated basis of axially symmetrical harmonic oscillator states. We would like to discuss the numerical checks which have been performed to test the stability of our

results with respect to the choice of the truncated basis.

For "ordinary" (time-even) HF calculations of equilibrium states, such a study consists mostly in making sure that the HF energy, the rms and the first multipole moments are reasonably well converged. For spherical nuclei, the "exact" calculation (in the coordinate space) allows us to know the degree of accuracy obtained for a given basis size, and to choose accordingly the number of oscillator shells. Let us notice that for spherical nuclei the scaling mass $M_{sc}(q)$, completely determined by the values of r_{st} [see Eqs. (2.1) to (2.3)], can be obtained from the exact $\vec{r}$ code for spherical nuclei, and is therefore given with an excellent accuracy. In CHF calculations of deformation energy curves, the physical energies to be considered are relative energies. The convergence therefore is ensured whenever increasing the basis size results roughly in a shift of the deformation energy curve as a whole. This is illustrated by Fig. 1 which shows for the ^{12}C nucleus a reasonable convergence with nine oscillator shells, the truncation error for the equilibrium energy being only 300 keV.

All the previous check do not ensure the convergence of the operator $\partial\rho_0/\partial q$ entering the time-odd constraining operator P. In this respect we have carefully studied the influence of the choice of the basis on the resulting mass parameters. The variation of the ^{12}C mass parameter at $q=0$

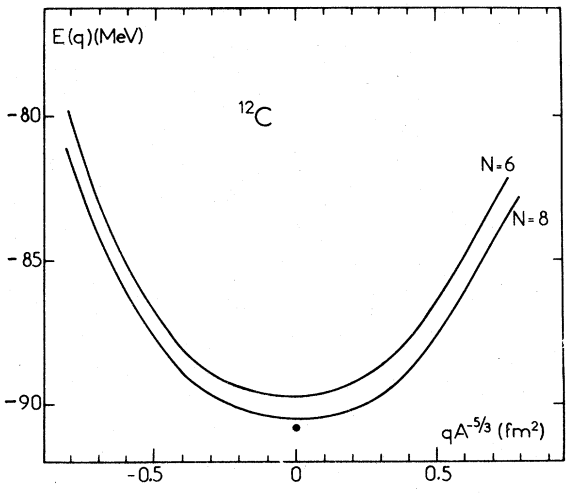

FIG. 1. Deformation energy curves of ^{12}C calculated with SIII for 7 and 9 oscillator shell basis. The "exact" result (obtained with an $\vec{r}$-space code) for the spherical configuration is represented by a dot. It is to be noted that in this figure, as in the following, N denotes the maximum total number of quanta in the harmonic oscillator basis.

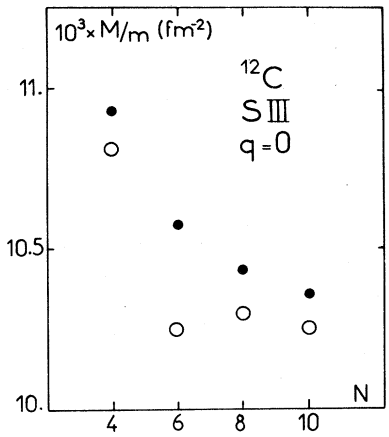

FIG. 2. Mass parameters of ^{12}C at spherical equilibrium, as functions of N. The dots represent self-consistent masses M_{CHF}, and the open circles correspond to cranking masses M_{ICR}.

with respect to the basis size is shown on Fig. 2. One sees that between 9 and 11 harmonic oscillator shells, both the self-consistent M_{CHF} and the Inglis cranking M_{ICR} mass parameters do not change more than by 1%. This study has been carried out with the same oscillator length for all basis sizes. Let us now investigate the combined effects on M_{CHF} of the oscillator parameter *and* the basis size. As is well known,[4] the optimal basis parameters (i.e., those minimizing the potential energy $E[\rho_0]$), may significantly change with the basis size. That is why on Figs. 3–5 we have plotted over a wide range of oscillator lengths the ^{16}O, ^{48}Ca, and ^{56}Ni mass parameters obtained at $q=0$ for basis including 5, 7, 9, and 11 oscillator shells. It has been found, for 9 or 11 oscillator shells, that the mass parameters are almost constant in a rather large interval of oscillator lengths around the optimal values. Moreover, the results obtained with 7, 9, or 11 oscillator shells are found to be very close, as already seen in the case of ^{12}C presented on Fig. 2.

One could think that all of this lengthy numerical

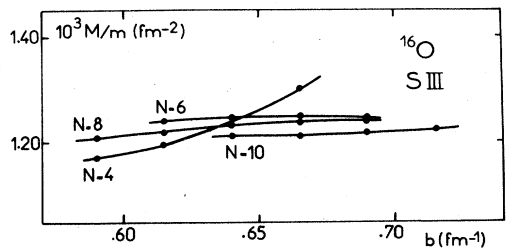

FIG. 3. Variations of the adiabatic mass M_{CHF} of ^{16}O with the oscillator constant $b=(m\omega/\hbar)^{1/2}$, for different basis sizes.

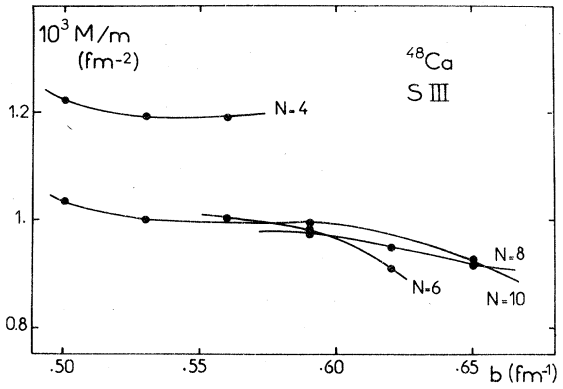

FIG. 4. Same as Fig. 3, for ^{48}Ca.

analysis could have been avoided by directly solving the double CHF equation in configuration space, as was done in Ref. 14. It must be remarked, however, that, in the present state of the art, such a solution in $\vec{r}$ space has only been achieved for a simplified Skyrme-like force without spin-orbit and without velocity-dependent parts. The first simplification prohibits a detailed description of dynamical properties for spin-unsaturated nuclei as ^{12}C and ^{56}Ni. The second restriction has the important consequence that the ATDHF mass reduces in this case to the Inglis cranking mass. Indeed, as shown by Eqs. (2.32) and (2.33), the time-odd HF potential W_1 arises for the Skyrme force only from its velocity-dependent part.

Let us now discuss the numerical evaluation of the operator $\partial\rho_0/\partial q$ for a given basis size. It has been computed from three CHF calculations of ρ_0 corresponding to the values $q_0 - dq$, q_0, $q_0 + dq'$ of the collective variable. For this purpose we have used a standard 3-points Lagrange formula:

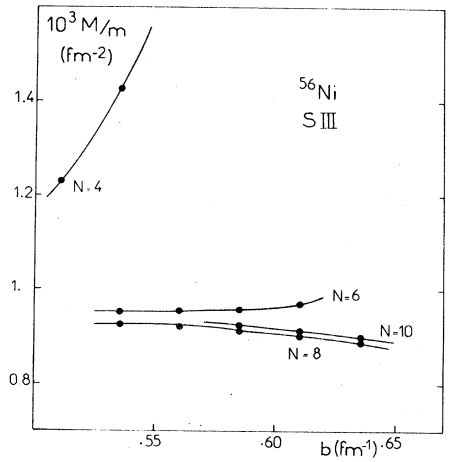

FIG. 5. Same as Fig. 3, for ^{56}Ni.

$$\left.\frac{\partial\rho_0}{\partial q}\right]_{q_0} = \frac{-dq'}{dq(dq+dq')}\rho_0(q_0-dq) + \frac{dq'-dq}{dqdq'}\rho_0(q_0) + \frac{dq}{dq'(dq+dq')}\rho_0(q_0+dq')\,. \tag{3.1}$$

In order to get reliable estimates for $\partial\rho_0/\partial q$ one must choose the magnitude of the differences dq, dq' in the collective variable not too small to yield significant numerical differences and not too large to guarantee the validity of the local quadratic behavior. The reliability of our choice for dq, dq' has been check by computations where these differences have been multiplied by 2 and $\frac{1}{2}$. In all cases the adiabatic mass parameters were found equal up to insignificant numerical differences.

The value of the collective velocity $\dot{q}$ should not be chosen too large (large enough though to secure numerical reliability) in order to ensure the linear response character of the solution. In Fig. 6 we have shown some quadrupole mass parameters as functions of the ratio of the adiabatic collective kinetic energy $\mathcal{K}$ [Eq. (2.32) of I] to the absolute value E of the ATDHF energy [Eq. (2.38) of I]. One sees that the linear response is obtained for a large range of collective velocities $\dot{q}$. In this figure, the arrows correspond to a crude estimate of the maximum collective velocities obtained in the nuclear ground state due to the quadrupole zero point motion. It is seen that for such maximum collective velocities, the linear response approximation is roughly valid.

It can also be noted that the smallness of $\dot{q}$ is

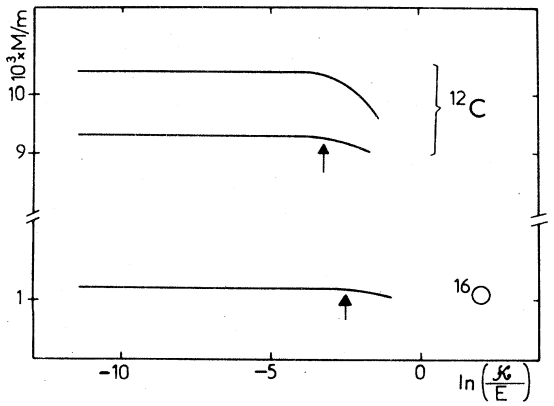

FIG. 6. Variation of the adiabatic mass M_{CHF} of ^{12}C and of ^{16}O with the collective velocity $\dot{q}$. The lower (upper) curve of ^{12}C corresponds to $A^{-5/3} = -0.56$ (0) fm^2 whereas for ^{16}O the calculation has been performed at $q = 0$. The choice of the abscissa (corresponding in fact to a linear plot in $\dot{q}$) is discussed in the text together with the meaning of the arrows.

TABLE I. Parameters of the SIII* and SVII forces. For both interactions, $x_3 = 1$ and $\alpha = 1$.

	t_0 (MeV fm^3)	t_1 (MeV fm^5)	t_2 (MeV fm^5)	t_3 (MeV fm^6)	x_0	x_1	x_2	W_0 (MeV fm^5)
SIII*	−1121	400	−533.33	14000	0.432 25	0.35	−0.9875	120
SVII	−1096.8	246.2	−148	17626	0.62	0	0	112

necessary for another reason; solving the double CHF problem does perturb the path given in Eq. (2.4) by terms of *second order in* $\dot{q}$. This comes from the effect of ρ_1 in the time-even part of Eq. (2.5) (see the discussion in Sec. IV of I). In the ^{40}Ca nucleus and for $\hbar\dot{q} = 0.1$ MeV fm^2 for instance, this modification of the path leads to relative variations of ATDHF energies, radii, and quadrupole moments smaller than 10^{-4}, 10^{-3}, and 10^{-2}, respectively, over a wide range of deformations.

The preceding discussion leads to the conclusion that our method is capable of yielding mass parameters with a very good accuracy. This is not surprising, since we calculate a nuclear polarizability (linear response to the external field P) by solving a Schrödinger equation only for occupied states. Computing mass parameters by perturbation techniques would require a description of unbound states, which are poorly represented in the oscillator basis.[15]

IV. RESULTS

In this section we present numerical results for the isoscalar axial quadrupole mode. Various effective forces have been used: (i) the SII*, SIII, SIV, and SV forces proposed in Ref. 5, (ii) a force called SVII, linearly extrapolated from the preceding to give a nuclear effective mass m^* equal to the nucleonic mass m, (iii) a force called SIII* with the same m^*/m ratio as SIII but where spin-stability properties have been slightly modified to improve some spectroscopic properties of the interaction,[16] and (iiii) the two forces *SG*0 [with the exponent α of Eq. (2.7) equal to either $\frac{1}{6}$ or to 1] proposed in Ref. 17. The parameters of all these forces can be found in Refs. 5 and 17, except for those of SIII* and SVII which are given in Table I.

Deformation energy curves obtained by CHF calculations in the vicinity of the spherical configuration are displayed on Fig. 7. The SIII force has been used for ^{12}C, ^{16}O, ^{40}Ca, and ^{56}Ni, and the SIV force also for ^{12}C and ^{16}O. In the ^{56}Ni case we have repeated the calculation with SIII* but the resulting energy curve cannot be distinguished from the SIII curve. To facilitate the comparison of curves corresponding to different nucleonic numbers A, we have plotted in abscissa throughout this paper, a "reduced" quadrupole moment $qA^{-5/3}$ in order to remove the trivial A dependence. In our HF (i.e., without pairing correlations) calculations, the range of deformation has been extended as far as the occurence of single-particle level crossings has permitted.

Figure 7 shows that ^{40}Ca is much stiffer against quadrupole deformation than ^{16}O and ^{56}Ni, whereas the ^{12}C nucleus appears to be very soft. Indeed, the distortion needed to gain 1 MeV is four times larger in ^{12}C than in ^{40}Ca. Notice the existence of a spherical equilibrium configuration for ^{12}C with SIII, while a very shallow valley centered around a negative q value is obtained with SIV. Therefore, by mere inspection of the *static* deformation energy curve one would infer a strong dependence of the ^{12}C ground state intrinsic deformation on the effective force. We will

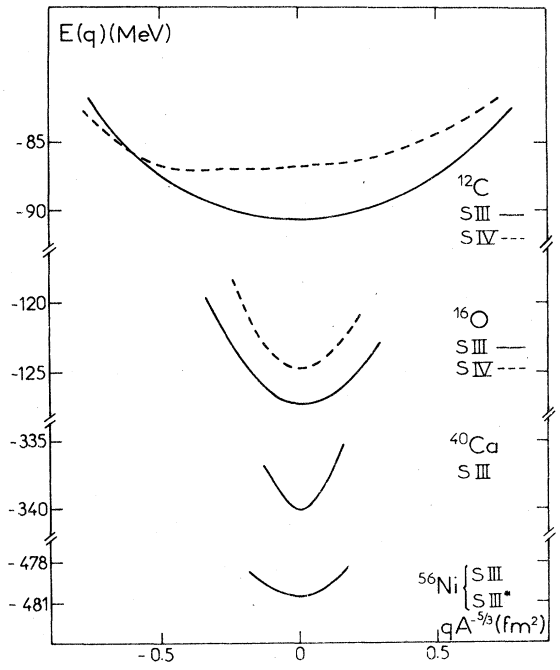

FIG. 7. Deformation energy curves of ^{12}C, ^{16}O, ^{40}Ca, and ^{56}Ni. SIV results are represented by dashed lines, and SIII results by solid lines. The SIII and SIII* forces lead, for ^{56}Ni, to the same curve.

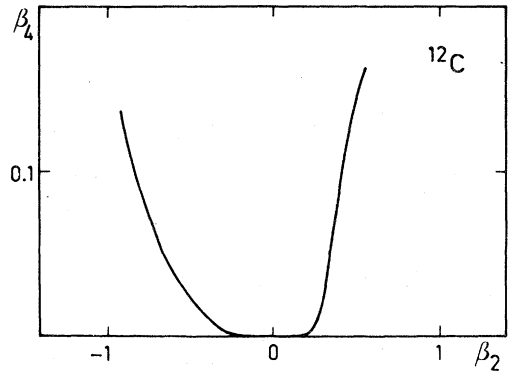

FIG. 8. Bohr and Mottelson standard deformation parameters of ^{12}C, calculated from SIII results for the CHF path.

see below that the (usually neglected) consideration of the associated adiabatic mass parameter can lead to a different conclusion.

It is interesting to analyze, in the ^{12}C case, the adiabatic path obtained from the solution of the CHF Eq. (2.4) with Q_{20} as constraining operator, in terms of quadrupole and hexadecapole surface distortions. For this purpose we have deduced the Bohr-Mottelson standard deformation parameters β_2 and β_4 from the calculated expectation values of the operators Q_{20} and Q_{40}. This has been done by assimilating the nuclear density with a sharply cut liquid-drop density. The result presented in Fig. 8 shows that for small quadrupole distortions ($|\beta_2| \leq 0.2$) the adiabatic path is well described in terms of Q_{20} surface deformation while this seems[18] not to be the case for larger $|\beta_2|$ values.

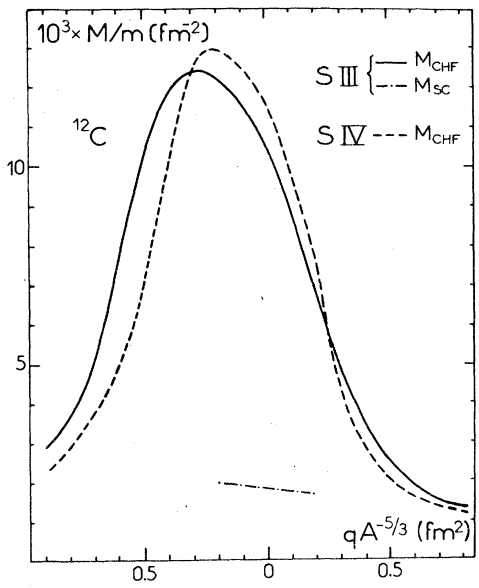

FIG. 9. Adiabatic mass parameters of ^{12}C, as functions of the collective variable. M_{CHF} is obtained from the CHF path with the constraint Q_{20}; M_{SC} is obtained from the scaling path (scaling with Q_{20} of a static HF solution).

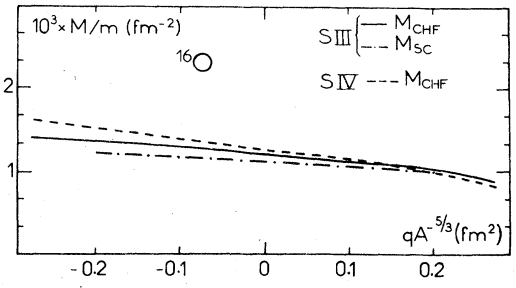

FIG. 10. Same as Fig. 9, for ^{16}O.

On Figs. 9–12 we show, for ^{12}C, ^{16}O, ^{40}Ca, and ^{56}Ni, the variation, with respect to the deformation, of the adiabatic mass for the CHF and scaling paths. For the latter we have limited (see the discussion of Sec. V in I) the range of $qA^{-5/3}$ to the interval $(-0.2, 0.2)$ corresponding to a maximum variation of the scaling parameter β of $\pm 1\%$. As expected from Eq. (2.1), the scaling mass parameters for all nuclei are smooth functions of q.

The mass parameters for CHF paths behave quite differently, their q variation has not the same features for spin-saturated nuclei (^{16}O, ^{40}Ca) as for spin-unsaturated nuclei (^{12}C, ^{56}Ni). For ^{16}O and ^{40}Ca, the HF masses are roughly constant with the deformation whereas for ^{12}C and ^{56}Ni they change dramatically. Such a well-marked structure is a clear-cut signature of anharmonic motion. Of particular significance is the bump in the mass of ^{12}C already reported in an earlier publication.[19] Recently, a very similar situation[14] has been encountered in the calculation of the quadrupole Inglis cranking mass associated with two colliding ^{12}C nuclei; a sharp peak has been found for a separation distance

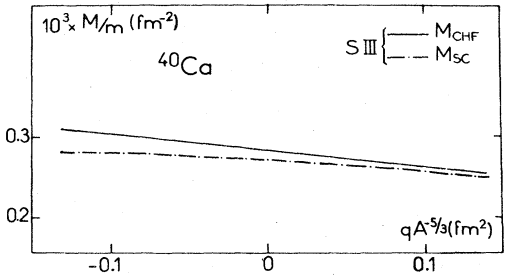

FIG. 11. Same as Fig. 9, for ^{40}Ca.

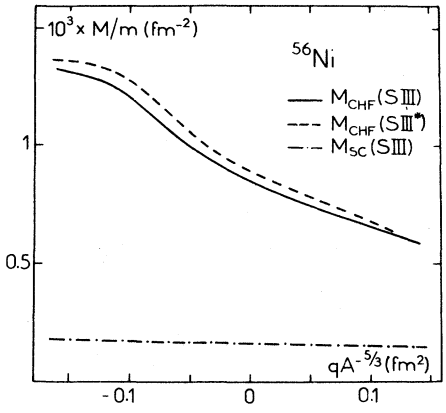

FIG. 12. Same as Fig. 9, for ^{56}Ni.

smaller than the barrier radius. In our case the behavior of the mass parameter can easily be explained. We first mention that in this case the Inglis cranking and self-consistent masses closely follow each other with an almost constant discrepancy of ~1–2% with the SIII force, and of ~3–4% with the SIV force. This allows us to restrict the discussion to the Inglis cranking mass:

$$M_{\mathrm{ICR}}(q)=\sum_{ph}\frac{|\langle p|\partial W_0/\partial q|h\rangle|^2}{\epsilon_{ph}^{\ 3}}. \tag{4.1}$$

The main contribution to Eq. (4.1) comes from the particle-hole excitation between the two $\Omega^\pi=\frac{1}{2}^-$ states stemming from the $1p^{3/2}$ and $1p^{1/2}$ spherical subshells as seen on Fig. 13. The minimum value of the corresponding particle-hole energy ϵ_{ph} occurs roughly at the same deformation as the bump in M_{ICR}. Moreover, the quantity $1/\epsilon_{ph}^{\ 3}$ roughly behaves, as a function of q, like M_{ICR} which implies that the matrix element in the numerator of Eq. (4.1) does not depend strongly on q.

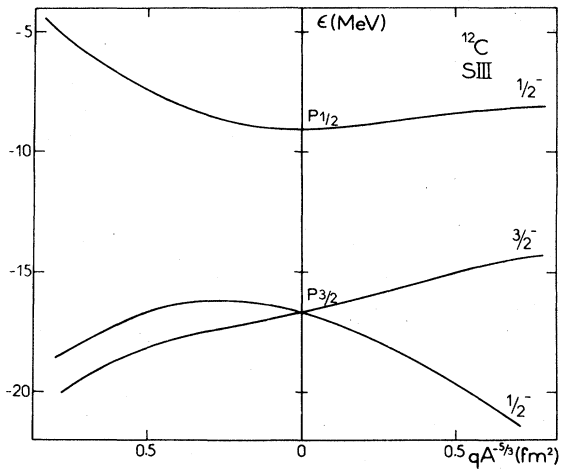

FIG. 13. Single-particle HF levels of ^{12}C around the Fermi surface as functions of the collective variable.

The spin-orbit splitting of the p shell results in an exchange (on the oblate deformation side of Fig. 13) of the two "asymptotic" [110] and [101] Nilsson $\Omega^\pi=\frac{1}{2}^-$ states, which is responsible, as we have seen, for the structure of the mass parameter. This kind of effect can thus be expected for all closed sub-shell nuclei which are not spin saturated. This is indeed the case for ^{56}Ni as seen on Fig. 12 where a similar structure as in ^{12}C takes shape. Unfortunately, due to the presence of level crossings, it has been impossible in this case to span the same range of deformation.

When requantizing the collective Hamiltonian with some quantization prescription one would therefore expect a concentration of the collective wave function around the deformation where the mass exhibits a maximum. This generates in the ^{12}C ground state an oblate deformation of purely dynamical origin. For ^{12}C and ^{56}Ni, the Bohr Hamiltonian is far from an harmonic oscillator one, which invalidates any small amplitude approximation.

As seen from Figs. 9 and 10, the mass parameters calculated for ^{12}C and ^{16}O with SIII and SIV, respectively, are very close. In particular the, same ground-state deformation of ^{12}C is found for both forces. In ^{56}Ni, SIII and SIII* yield also adiabatic masses in very good agreement (one expects, however, more important differences for *isovector* modes).

On Table II we present the quadrupole mass parameters calculated[20] at $q=0$ with SIII for both scaling and CHF paths. To facilitate the comparison between different nuclei we have multiplied the mass parameters by $A^{5/3}$. As expected, the "reduced" scaling masses are found almost constant with A. Indeed, since they correspond to an irrotational flow motion, their variation with A must go as $A^{-5/3}$. In contrast, the "reduced" CHF masses display a significant A dependence. For magic light (i.e., spin-saturated) nuclei they are equal to (or slightly larger than) the corresponding scaling values; for nonmagic nuclei they are much larger. This is easily understood in terms of random phase approximation (RPA) sum rules (see Sec. VI of I). For nuclei with static equilibrium at $q=0$, we know for the scaling mass $M_{\mathrm{SC}}(q=0)$ that

$$M_{\mathrm{SC}}(q=0)=\frac{\hbar^2}{2}\frac{1}{m_1(Q_{20})}, \tag{4.2}$$

whereas for the CHF mass $M_{\mathrm{CHF}}(q=0)$,

$$M_{\mathrm{CHF}}(q=0)=\frac{\hbar^2}{2}\frac{m_{-3}(Q_{20})}{[m_{-1}(Q_{20})]^2}. \tag{4.3}$$

TABLE II. Mass parameters of various nuclei at spherical equilibrium, in reduced units $MA^{5/3}$, for the CHF and scaling paths, calculated with SIII.

	^{12}C	^{16}O	^{40}Ca	^{48}Ca	^{56}Ni	^{90}Zr	^{140}Ce	^{208}Pb
$\frac{M_{CHF}\ (q=0)}{m} \times A^{5/3}$ (fm^{-2})	0.65	0.13	0.13	0.60	0.72	0.32	0.17	0.25
$\frac{M_{SC}\ (q=0)}{m} \times A^{5/3}$ (fm^{-2})	0.13	0.12	0.13	0.13	0.14	0.14	0.14	0.14

As mentioned in I these masses satisfy

$$M_{CHF}\ (q=0) \geq M_{SC}(q=0)\,, \tag{4.4}$$

which is verified in our calculations (see Table II). Moreover, the large discrepancies between M_{CHF} and M_{SC}, when they occur, are clearly related to a distribution of the quadrupole strength between "0-$\hbar\omega$" and "2-$\hbar\omega$" particle-hole excitations. This is obviously the case for open-shell nuclei. For heavy magic nuclei, the spin-orbit coupling, as is well known, introduces in the hole states, intruder orbitals from the next shell (which gives rise to low-lying states in the RPA spectrum). On the contrary, the two masses are roughly equal for light magic nuclei, where 0-$\hbar\omega$ excitations are forbidden by the Pauli principle.

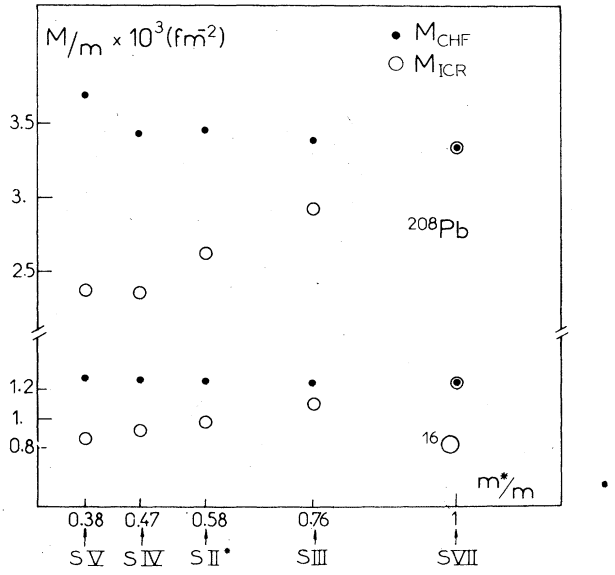

FIG. 14. Mass parameters of ^{208}Pb and ^{16}O (at spherical equilibrium) as functions of the interactions characterized by their effective mass. The dots represent self-consistent masses M_{CHF}, and the open circles correspond to cranking masses M_{ICR}.

Restricting ourselves from now on to the CHF path, we shall compare the exact adiabatic mass M_{CHF} with its non-self-consistent (Inglis cranking) approximation M_{ICR}. In fact, it is mainly for this purpose that various Skyrme forces all yielding the same saturation properties but having different effective masses m^* have been used. By inspection of Eq. (2.29) defining m^* and Eqs. (2.32) and (2.33) defining $W_1(\vec{r})$, one sees that for isoscalar modes (assuming moreover that $\rho^q = \rho/2$ and $\vec{j}^q = \vec{j}/2$) the time-odd self-consistent field $W_1(\vec{r})$ is proportional to $(m/m^* - 1)$. One expects therefore the difference ΔM

$$\Delta M = M_{CHF} - M_{ICR} \tag{4.5}$$

to be a monotonous function of $(m/m^* - 1)$. This is illustrated in Fig. 14. ΔM decreases with m^*/m for ^{16}O and ^{208}Pb; one notices also that $\Delta M = 0$ for SVII, for which $m^* = m$. As seen on Fig. 15 for ^{16}O, $\Delta M/M_{ICR}$ is also an increasing function of $(m/m^* - 1)$ and varies between 0 and 50% for all considered Skyrme forces. Since the ef-

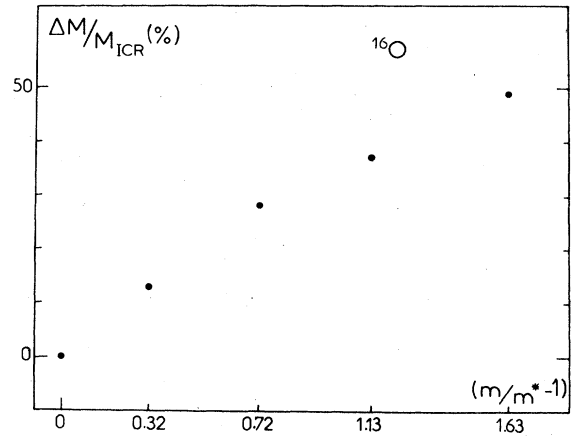

FIG. 15. Relative discrepancy between self-consistent (M_{CHF}) and cranking (M_{ICR}) mass parameters, as function of the interactions [characterized by the function $(m/m^* - 1)$ of their effective mass m^*], for ^{16}O at spherical equilibrium.

TABLE III. Relative discrepancy between self-consistent (M_{CHF}) and cranking (M_{ICR}) mass parameters for various nuclei at spherical equilibrium, calculated with SIII.

	^{12}C	^{16}O	^{40}Ca	^{48}Ca	^{56}Ni	^{90}Zr	^{140}Ce	^{208}Pb
$\Delta M/M_{ICR}$ $(q=0)$ (%)	1	11	8	7	13	11	10	16

fective mass in nuclear matter is expected[6,21] to be of the order of $(0.6-0.8)m$, one is led to assess a validity of ~15–30% to the mass parameters calculated with the Inglis cranking formula (at least for the isoscalar quadrupole mode). This is illustrated by Table III where $\Delta M/M_{ICR}$ is given for various nuclei calculated (at $q=0$) with SIII.

For ^{16}O, we have calculated M_{CHF} and M_{ICR} with the two forces SG0 of Ref. 17, corresponding to different powers of ρ ($\alpha=1$ and $\frac{1}{6}$) in the density-dependent force, both having the same effective mass $m^*/m=0.64$. Results displayed in Table IV show that $\Delta M/M_{ICR}$ is the same for the two forces. Moreover, these interactions lead, for M_{CHF}, to the same value as the other Skyrme forces (see Fig. 14); also, the result for M_{ICR} would take place in Fig. 14, on the straight line joining the points. These results and the result in ^{56}Ni with SIII* show that the value of m^* is the relevant parameter to characterize the degree of validity of the Inglis cranking formula. {Indeed, in this respect, the dependence of the path ρ_0 and of the currents $\vec{j}^q$ [see Eqs. (2.32) and (2.33)] on the choice of the interaction does not seem to play any role.}

It has been found in extensive calculations (with SIII and SIV for ^{12}C, ^{16}O, and ^{40}Ca) that ΔM is roughly constant with q. This seems to indicate that, at least for the isoscalar quadrupole mode, the effect of self-consistency is merely to shift upwards the curve $M_{ICR}(q)$.

We come now to an interesting feature which can be observed for ^{16}O on Fig. 14 and which is the quasiconstancy of $M_{CHF}(q=0)$ with respect to m^*, in contrast to the strong variation of M_{ICR}. Indeed, why M_{ICR} is an increasing function of m^* is easy to explain, since to increase m^* amounts to contract the single-particle spectrum, and hence to decrease the energy denominators in Eq. (4.1). The explanation of the quasiconstancy of $M_{CHF}(q=0)$ is somewhat more subtle. Take the magic ^{16}O nucleus; in this case the quadrupole strength is concentrated in the narrow giant resonance and the sum rule inequalities [Eq. (6.4)] of I become

$$\frac{m_3(Q_{20})}{m_1(Q_{20})}\simeq\frac{m_1(Q_{20})}{m_{-1}(Q_{20})}\simeq\frac{m_{-1}(Q_{20})}{m_{-3}(Q_{20})}. \tag{4.6}$$

On the other hand, it is known[22] that for Skyrme forces

$$m_3(Q_{20})\propto(m^*)^{-1}, \tag{4.7}$$

and also that $m_1(Q_{20})$ is almost constant with m^* (which comes from the force parameter adjustment to a correct saturation density). Therefore, Eq. (4.6) leads to

$$\begin{aligned} m_{-1}(Q_{20})&\propto m^*,\\ m_{-3}(Q_{20})&\propto(m^*)^2, \end{aligned} \tag{4.8}$$

which shows, according to Eq. (4.3), the independence of M_{CHF} on m^*.

This argument, which was developed for ^{16}O, cannot be applied to ^{208}Pb where the quadrupole strength is more fragmented and indeed a slight but significant dependence of M_{CHF} on m^* is found in this case (see Fig. 14).

TABLE IV. Self-consistent (M_{CHF}) and cranking (M_{ICR}) mass parameters of ^{16}O at spherical equilibrium, calculated with the SG0 forces (characterized by the exponent α of ρ in the density-dependent term).

α	$10^3M_{ICR}/m$ (fm^{-2})	$10^3M_{CHF}/m$ (fm^{-2})	$\Delta M/M_{ICR}$
1	1.06	1.28	21%
$\frac{1}{6}$	1.01	1.22	21%

V. CONCLUSION

In the present works (papers I and II), we have carried out a theoretical study of the ATDHF formalism when it is restricted to a single collective trajectory, assumed to be known, together with a practical application to a specified collective motion, the quadrupole mode.

Two possible choices for the adiabatic paths have been considered. For the standard scaling path, we have found an analytical solution of the first set of Hamilton equations, which directly provides the mass parameter. To be able to compare the scaling mass with the CHF one, we have chosen the same collective variable in the

two cases, which restricts the scaling transformation to small amplitude motions. In the CHF path case, we have developed a method to calculate the mass parameter, which reduces to a doubly constrained HF problem. This method avoids difficulties in dealing explicitly with the continuum part of the HF spectrum (as encountered in perturbation series), since it is equivalent to the solution of the Schrödinger equation for bound states. As shown by our numerical applications, the resulting values of the mass parameters are quite reliable, even if the solution is performed in a truncated harmonic oscillator basis.

This doubly constrained HF form of the first ATDHF equation is reminiscent of the starting points of other approaches to collective motion. In some of these, one chooses a time-even constraining operator Q defining the path (as we do), but there is no unique prescription to define the time-odd constraint P generating the dynamics. In our case, the operator P is unequivocally defined (except for irrelevant diagonal matrix elements) by the first Hamilton equation of motion. For any kind of path, the "coordinate" Q and the "momentum" P satisfy weak quantal canonical relations and their expectation values with respect to the time-dependent wave function are classically conjugate.

Numerical calculations of mass parameters have been performed for the two paths, with Q_{20} as scaling or constraining operator. Several interactions of the Skyrme type have been used. We have in particular focused our attention on four points: (i) distinction between small and large amplitude motions, (ii) comparison of the two choices of the path, (iii) for the CHF path, comparison between the ATDHF and the Inglis cranking masses, and (iv) influence on the results of the choice of the interaction (among a family of saturating Skyrme forces).

As is well known, the scaling path leads to the irrotational hydrodynamical value for the mass parameter. In reduced units ($MA^{5/3}$), this mass at equilibrium has almost the same value for all spherical nuclei (indeed, it is proportional to the inverse square of the nucleus radius). The scaling path is appropriate for the description of giant resonances, since it provides the excitation energy $E_3=(m_3/m_1)^{1/2}$, which is almost insensitive to the low-lying part of the spectrum. On the contrary, the CHF path does contain information on the shell structure; this is illustrated by the value $\frac{1}{2}\hbar^2 m_{-3}/(m_{-1})^2$ of the inertial parameter, which is dominated by the low energy states. Consequently, the CHF path, with Q_{20} as the constraint, is more appropriate to describe low energy collective excitations. For doubly closed shell nuclei it happens, however, that this path is capable of describing the giant resonance. In this case, which is a case of RPA harmonic vibrations, the CHF mass parameter is roughly constant with respect to the deformation, and very close to the scaling mass.

For non-spin-saturated nuclei (see the results for ^{12}C and ^{56}Ni), the CHF mass parameter exhibits a strong structure with respect to the deformation. This is incompatible with a small amplitude motion, and is a signature of the occurrence of anharmonic effects.

A systematic study of the results at the equilibrium spherical state shows that the ATDHF mass parameter is nearly independent of the choice of the Skyrme interaction. For light doubly closed shell nuclei, this quasiconsistancy can be proved analytically in terms of sum rules. On the contrary, the cranking mass is very sentitive to the interaction, and this sensitivity appears therefore to be a spurious effect due to the lack of self-consistency. In this respect, all the tests carried out with a large variety of Skyrme-like forces lead to the conclusion that the relevant parameter is the effective mass m^* in nuclear matter. For "reasonable" values of m^* (as in SIII), the self-consistent and cranking inertial parameter differ by 15–30%.

However, one should not extrapolate these results to other kinds of collective excitations, and, in particular, to rotational spectra. Relaxing some symmetries would give rise to new terms in the time-odd field W_1, leading possibly to a quite different value of the ratio $(M_{\mathrm{CHF}}-M_{\mathrm{ICR}})/M_{\mathrm{ICR}}$. Moreover, it would remain to investigate the effects of the other parametrizations of the effective interactions.

In the present work we have ignored the question of determining microscopically the adiabatic path. To solve this problem one would encounter, as in "exact" TDHF calculations, the difficulty of finding (or even averaging over) initial conditions. Some attempts to determine the collective paths have been proposed.[23-25] But in practice, they involve a considerable amount of difficulties. In our opinion it is not clear that such approaches are more valuable than extracting the path from TDHF solutions in the adiabatic limit.[26] It should also be stressed that, up to now, the numerical applications of all these methods are restricted to effective forces which are not as elaborate as those used in this paper. (In particular, the inclusion of the spin-orbit force is needed to describe low energy collective motion).

The method presented here and illustrated by a lot of numerical calculations is both practicable

and microscopically well founded. In many respects however (the choice of the path, the absence of pairing correlations, the single collective variable reduction, etc.) there is room for further improvements.

ACKNOWLEDGMENTS

This work would not have been completed without constant and fruitful interaction with M. Vénéroni. We would like to express our gratitude to him and to D. Vautherin, for stimulating discussions and a critical reading of the manuscript. For the question of symmetries we have benefitted from the help of D. Vautherin and from a constructive criticism of J. Dobaczewski and A. Sobiczewski. We are indebted to X. Campi and H. Flocard for valuable discussions. We thank also D. Vautherin and F. Moreau for their contribution to the first stage of the numerical calculations. Finally, the Bureau de Calcul (IPN, Orsay) is gratefully acknowledged for extended computing facilities. This work has been performed at the Division de Physique Théorique (Institut de Physique Nucléaire), which is Laboratoire associé au C. N. R. S.

APPENDIX A: GAUGE INVARIANCE OF THE SKYRME FORCE WITH RESPECT TO ISOSCALAR SPIN-INDEPENDENT OPERATORS

(1) *Definition.* Given any wave function $|\phi_0\rangle$ and a Hermitian operator Q defining a new wave function $|\phi\rangle$ by

$$|\phi\rangle = e^{iQ}|\phi_0\rangle\,, \tag{A1}$$

the interaction V is said to be gauge invariant with respect to Q if

$$\langle\phi_0|V|\phi_0\rangle = \langle\phi|V|\phi\rangle = \langle\phi_0|e^{-iQ}Ve^{iQ}|\phi_0\rangle\,. \tag{A2}$$

A sufficient condition for that is

$$[V,Q]=0\,, \tag{A3}$$

as can be readily seen by expanding the exponentials. It may be noted that if $|\phi_0\rangle$, V, and Q are all time-even objects, the less restrictive condition[27]

$$[Q,[Q,V]]=0 \tag{A4}$$

is sufficient, the expectation value of time-odd operators vanishing for time-even states.

(2) *The Central Skyrme force.* Let us restrict ourselves for the moment to the central part of the two-body Skyrme force. If the spin-independent operator Q commutes with the spatial part of the central force, the whole central force is obviously gauge invariant (including the exchange terms). That is why we can limit ourselves to the gauge invariance property of the spatial part of the central force, the following proof being partially borrowed from Refs. 21 and 28.

The velocity-independent part

$$V_0(\vec{r}_1,\vec{r}_2)=\left[C+Df\left(\frac{\vec{r}_1+\vec{r}_2}{2}\right)\right]\delta(\vec{r}_1-\vec{r}_2) \tag{A5}$$

of the Skyrme force fulfills obviously the condition (A3). We are then left with two interaction terms

$$V_1=\sum_{ij}(\vec{P}_{ij}{}^2\delta_{ij}+\delta_{ij}\vec{P}_{ij}{}^2) \tag{A6}$$

and

$$V_2=\sum_{ij}(\vec{P}_{ij}\cdot\delta_{ij}\vec{P}_{ij}) \tag{A7}$$

with the notation

$$\begin{aligned}&\delta_{ij}=\delta(\vec{r}_i-\vec{r}_j)\,,\\ &\vec{P}_{ij}=\vec{P}_i-\vec{P}_j\,,\\ &\vec{P}_j=\frac{\hbar}{i}\vec{\nabla}_j\,.\end{aligned} \tag{A8}$$

The definitions (A6) and (A7) of the velocity-dependent parts of the Skyrme force differ from Eq. (2.7) by the replacement of $\vec{P}'$ by $\vec{P}$, which is irrelevant for our purpose here [the same remark holds for Eq. (A17) below].

From now on we will restrict ourselves to a one-dimensional problem since V_1 and V_2 involve only scalar products. It is easily seen that

$$[P_{ij},\delta_{ij}^{(n)}]=\frac{2\hbar}{i}\delta_{ij}^{(n+1)}\,, \tag{A9}$$

where $\delta^{(n)}$ is the nth derivative of δ. Moreover, upon defining

$$Q=\sum_{k=1}^{A}q(\vec{r}_k)=\sum_{k=1}^{A}q_k\,, \tag{A10}$$

one gets readily

$$[q_k,\delta_{ij}^{(n)}]=0\,. \tag{A11}$$

It is now possible to prove that if V_2 commutes with Q, V_1 does it also, since

$$\begin{aligned}[P_{ij}{}^2\delta_{ij}+\delta_{ij}P_{ij}{}^2,q_k]&=\left[2P_{ij}\delta_{ij}P_{ij}+\frac{2\hbar}{i}[P_{ij},\delta_{ij}^{(1)}],q_k\right]\\ &=2[P_{ij}\delta_{ij}P_{ij},q_k]-(2\hbar)^2[\delta_{ij}^{(2)},q_k]\\ &=2[P_{ij}\delta_{ij}P_{ij},q_k]\,.\end{aligned} \tag{A12}$$

To demonstrate that V_2 commutes with Q, one first notes, using Eqs. (A9) and (A11), that

$$[P_{ij}\delta_{ij}P_{ij},q_k]=[P_{ij},[P_{ij},q_k]\delta_{ij}]_+\,. \tag{A13}$$

Now since

$$[P_{ij}, q_k] = \begin{cases} \frac{2\hbar}{i} q_k^{(1)} & \text{if } i=k \\ -\frac{2\hbar}{i} q_k^{(1)} & \text{if } j=k \\ 0 & \text{otherwise,} \end{cases} \tag{A14}$$

one gets

$$[V_2, Q] = \frac{4\hbar}{i} \sum_{jk} [P_{kj}, q_k^{(1)} \delta_{kj}]_+ . \tag{A15}$$

Partially resumming the (j,k) and (k,j) contributions, one sees that $[V_2, Q]$ vanishes since $P_{kj} = -P_{jk}$ and $q_k^{(1)}\delta_{kj} = q_j^{(1)}\delta_{jk}$. As seen in Eq. (A10), we have considered an *isoscalar* operator Q. An *isovector* operator Q would have been defined as

$$Q = \sum_k \epsilon_k q_k \tag{A16}$$

with, e.g., $\epsilon_k = 1$ for protons, $\epsilon_k = -1$ for neutrons, and the previous proof could have been repeated up to Eq. (A15), the cancellation of the (j,k) and (k,j) contributions occuring only for $\epsilon_k = \epsilon_j$. As a result, the velocity-dependent Skyrme force is generally not gauge invariant with respect to isovector operators Q, as already noted in Refs. 7, 21, and 29.

(3) *The spin orbit force.* Let us consider the interaction

$$V_{so} = \sum_{ij} (\vec{P}_{ij} \times \delta_{ij} \vec{P}_{ij}) \cdot (\vec{\sigma}_i + \vec{\sigma}_j) . \tag{A17}$$

Using Eq. (A9), the x component of $\vec{P}_{ij} \times \delta_{ij} \vec{P}_{ij}$ writes

$$(\vec{P}_{ij} \times \delta_{ij} \vec{P}_{ij})^x = \frac{2\hbar}{i} (P_{ij}^z \delta_{ij}^{\prime y} - P_{ij}^y \delta_{ij}^{\prime z}) , \tag{A18}$$

where P_{ij}^z is the z component of P_{ij} and $\delta_{ij}^{\prime y}$ the first partial derivative of δ_{ij} with respect to y. From Eqs. (A14) and (A18) one gets

$$\sum_{ijk} [(\vec{P}_{ij} \times \delta_{ij} \vec{P}_{ij})^x, q_k] = -4\hbar^2 \sum_{jk} (\delta_{kj}^{\prime y} q_k^{\prime z} + \delta_{jk}^{\prime z} q_k^{\prime y}) , \tag{A19}$$

where $q_k^{\prime z}$ is the first partial derivative of q_k with respect to z. Collecting the contributions from the pairs (k,j) and (j,k) leads to the vanishing of the commutator (A19). A similar demonstration for the y and z components would achieve the proof of the gauge invariance of V_{so} with respect to isoscalar operators Q.

(4) *The Coulomb force.* Since the Coulomb force is velocity independent, it is gauge invariant with respect to isoscalar operators. It is trivial to show that this is also true for isovector operators.

APPENDIX B: WAVE FUNCTIONS AND IMPOSED SYMMETRIES

Consider a one-body reduced density matrix ρ commuting with J_3 and P_0, and define occupied states of ρ which are eigenstates of J_3 and P_0 with eigenvalues Ω and π. Their wave function in cylindrical coordinates can be written as

$$\varphi(\vec{r}, \vec{\sigma}) = \phi^-(r,z) e^{i\Lambda^+\theta} |-\rangle + \phi^+(r,z) e^{i\Lambda^-\theta} |+\rangle , \tag{B1}$$

where

$$\Lambda^\pm = \Omega \pm \tfrac{1}{2} , \tag{B2}$$

and where the kets $|\pm\rangle$ are the eigenstates of s_3.

Let us define for each φ, a state $\tilde{\varphi} = U_2 \varphi$ which is another occupied state of ρ with the wave function[30]

$$\tilde{\varphi}(\vec{r}, \vec{\sigma}) = \phi^-(r,z) e^{-i\Lambda^+\theta} |+\rangle - \phi^+(r,z) e^{-i\Lambda^-\theta} |-\rangle . \tag{B3}$$

It is an eigenstate of J_3 and P_0 with eigenvalues $-\Omega$ and π.

Let us introduce also the state $\bar{\varphi}$ deduced from φ by time-reversal conjugation $\mathcal{C}$:

$$\bar{\varphi}(\vec{r}, \vec{\sigma}) = -\phi^-(r,z)^* e^{-i\Lambda^+\theta} |-\rangle + \phi^+(r,z)^* e^{-i\Lambda^-\theta} |+\rangle . \tag{B4}$$

Time-even densities. If in addition to the J_3 and P_0 symmetries we assume that ρ is even under time reversal, there exists a representation which is such that the functions ϕ^- and ϕ^+ are real and therefore

$$\tilde{\varphi} = -\bar{\varphi} . \tag{B5}$$

Hence, since ρ commutes with $\mathcal{C}$ it commutes also with U_2.

Consequence of the U_2 symmetry on density functions. It is easy to check that the wave functions φ and $\tilde{\varphi}$ and defined in Eqs. (B1) and (B3) give the same contribution to the spin-scalar density functions ρ, τ, j_r, j_z, and $\vec{\nabla} \cdot \vec{J}$.

APPENDIX C: THE SYMMETRIES OF THE SOLUTIONS INDUCE THE VANISHING OF SOME DENSITIES

First we show that the spin-vector density matrix $\vec{\rho}$ vanishes when the symmetries (i), (ii), and (iii) defined in Sec. II C are assumed. Any vector $\vec{V}$ will be represented by its *cylindrical* coordinates V_k $(k = r, \theta, z)$ defined from the Cartesian representation V_1, V_2, V_3 by

$$V_r=\tfrac{1}{2}(V_+e^{-i\theta}+V_-e^{i\theta}),$$
$$V_\theta=\tfrac{1}{2}i(-V_+e^{-i\theta}+V_-e^{i\theta}), \quad \text{(C1)}$$
$$V_z=V_3,$$

where

$$V_\pm=V_1\pm iV_2. \quad \text{(C2)}$$

Let us denote by $\rho^{(l)}$ the density matrix

$$\rho^{(l)}=U_l\rho. \quad \text{(C3)}$$

From the symmetry properties

$$[\vec{\rho},U_l]=0, \quad \text{(C4)}$$

and therefore

$$\rho_k^{(l)}=\rho_k, \quad k=r,\theta,z. \quad \text{(C5)}$$

To prove the vanishing of $\vec{\rho}$ we will show by explicit action of a suitably chosen U_l transformation that

$$\rho_k^{(l)}=-\rho_k, \quad k=r,\theta,z. \quad \text{(C6)}$$

r component. Let us consider the action of U_3 on ρ_r

$$\rho_r^{(3)}(\vec{x},\vec{x}')=\sum_{\sigma\sigma'}\langle r,z,\theta,\sigma|U_3^+\rho U_3|r',z',\theta',\sigma'\rangle \times\langle\sigma'|\sigma_r|\sigma\rangle, \quad \text{(C7)}$$

where

$$U_3=P_0e^{i\pi I_3}i\sigma_3$$

and

$\vec{x}(\vec{x}')$ stands for $r,z,\theta(r',z',\theta')$.

The $P_0e^{i\pi I_3}$ operator transforms (r,z,θ) into $(r,-z,\theta)$. Since the density matrix is invariant under this transformation, its radial part is even with respect to z and therefore

$$\rho_r^{(3)}(\vec{x},\vec{x}')=\sum_{\sigma\sigma'}\langle\vec{x},\sigma|\sigma_3\rho\sigma_3|\vec{x}',\sigma'\rangle\langle\sigma'|\sigma_r|\sigma\rangle. \quad \text{(C8)}$$

Defining

$$|\tilde{\sigma}\rangle=\sigma_3|\sigma\rangle \quad \text{(C9)}$$

and similarly

$$|\tilde{\sigma}'\rangle=\sigma_3|\sigma'\rangle \quad \text{(C10)}$$

leads to

$$\rho_r^{(3)}(\vec{x},\vec{x}')=\sum_{\sigma\sigma'}\langle\vec{x},\tilde{\sigma}|\rho|\vec{x}',\tilde{\sigma}'\rangle\langle\tilde{\sigma}'|\sigma_3\sigma_r\sigma_3|\tilde{\sigma}\rangle. \quad \text{(C11)}$$

Since

$$\sigma_3\sigma_r\sigma_3=-\sigma_r, \quad \text{(C12)}$$

one easily gets

$$\rho_r^{(3)}(\vec{x},\vec{x}')=-\rho_r(\vec{x},\vec{x}'). \quad \text{(C13)}$$

θ component. A similar proof for ρ_θ gives

$$\rho_\theta^{(3)}(\vec{x},\vec{x}')=-\rho_\theta(\vec{x},\vec{x}'). \quad \text{(C14)}$$

z component. In this case we consider the action of U_2 on ρ_z. The operator $P_0e^{i\pi I_2}$ transforms (r,z,θ) into $(r,z,-\theta)$. Due to the axial symmetry the radial part of ρ_z does not depend on θ and therefore

$$\rho_z^{(2)}(\vec{x},\vec{x}')=\sum_{\sigma\sigma'}\langle\vec{x},\sigma|\sigma_2\rho\sigma_2|\vec{x}',\sigma'\rangle\langle\sigma'|\sigma_z|\sigma\rangle. \quad \text{(C15)}$$

From

$$\sigma_2\sigma_z\sigma_2=-\sigma_z, \quad \text{(C16)}$$

one gets readily

$$\rho_z^{(2)}(\vec{x},\vec{x}')=-\rho_z(\vec{x},\vec{x}'). \quad \text{(C17)}$$

Extension to other density functions. The preceding arguments can easily be extended to demonstrate the vanishing of the kinetic energy spin-vector density $\vec{\tau}$, the scalar part of the $J_{\mu\nu}$ tensor, and the j_θ component of the current vector $\vec{j}$.

APPENDIX D: THE MATRIX ELEMENTS OF W_1 IN THE HARMONIC OSCILLATOR BASIS

(1) *Notation.* A normalized basis vector is defined by two oscillator constants $c_\perp$ and c_z and by a set of 4 quantum numbers n_z, $n_\perp$, Λ,Σ, eigenvalues of the numbers of quanta in the z direction and in the $x0y$ plane, the z component of the orbital and spin angular momenta (divided by $\hbar$), respectively. One generally introduces

$$n=\tfrac{1}{2}(n_\perp-|\Lambda|) \quad \text{(D1)}$$

and defines the current basis vector by $\alpha\equiv\{n_z,n,\Lambda,\Sigma\}$. In cylindrical coordinates (r,θ,z) the corresponding normalized spatial wave function can be expressed as the product of three wave functions:

$$\varphi_{n_z n,\Lambda}(\vec{r})=\psi_n^\Lambda(r)\psi_{n_z}(z)\psi_\Lambda(\theta). \quad \text{(D2)}$$

The radial wave function (for $\Lambda>0$) writes

$$\psi_n^\Lambda=N_n^\Lambda c_\perp\sqrt{2}\,\eta^{\Lambda/2}e^{-\eta/2}L_n^\Lambda(\eta), \quad \text{(D3)}$$

with

$$N_n^\Lambda=\left[\frac{n!}{(n+\Lambda)!}\right]^{1/2} \quad \text{(D4)}$$

and

$$\eta=c_\perp^2r^2, \quad \text{(D5)}$$

$L_n^\Lambda(x)$ being the usual Laguerre polynomial.[31] The longitudinal wave function writes

$$\psi_{n_z} = M_{n_z}\sqrt{c_z}\,e^{-\xi^2/2}H_{n_z}(\xi), \tag{D6}$$

where

$$M_{n_z} = (\sqrt{\pi}\,2^{n_z}n_z!)^{-1/2} \tag{D7}$$

and

$$\xi = c_z z, \tag{D8}$$

$H_{n_z}(x)$ being the usual Hermite polynomial.[31] The angular wave function writes

$$\psi_\Lambda = \frac{1}{\sqrt{2\pi}}e^{i\Lambda\theta}. \tag{D9}$$

To deal with first derivatives of the ψ's we introduce as in Ref. 3 new polynomials $\bar{H}_{n_z}$ and $\bar{L}_n^\Lambda$ defined by

$$\nabla_z\psi_{n_z}(\xi) = M_{n_z}c_z^{3/2}e^{-\xi^2/2}\bar{H}_{n_z}(\xi), \tag{D10}$$

$$\nabla_r\psi_n{}^\Lambda(r) = N_n^\Lambda c_\perp{}^2\sqrt{2}\,\eta^{(\Lambda-1)/2}\bar{L}_n^\Lambda(\eta). \tag{D11}$$

Using standard relations for H and L polynomials leads to

$$\bar{H}_{n_z}(\xi) = \xi H_{n_z}(\xi) - H_{n_z+1}(\xi), \tag{D12}$$

$$\bar{L}_n^\Lambda(\eta) = 2(n+1)L_{n+1}^\Lambda(\eta) - (2n+\Lambda+2-\eta)L_n^\Lambda(\eta). \tag{D13}$$

(2) *Current.* The k component of the current vector $\vec{j}$ can be written in terms of the basis wave functions φ_α and $\varphi_{\alpha'}$ as

$$j_k(\vec{r}) = \frac{1}{2i}\sum_{\alpha\alpha'}[\rho_{\alpha\alpha'}\nabla_k\varphi_\alpha(\vec{r})\varphi_{\alpha'}^*(\vec{r}) - \varphi_\alpha(\vec{r})\nabla_k\varphi_{\alpha'}^*(\vec{r})]. \tag{D14}$$

Using the Hermiticity of ρ and the reality of $\nabla_k\varphi_\alpha(\vec{r})\varphi_{\alpha'}^*(\vec{r})$ ($\Lambda_\alpha = \Lambda_{\alpha'}$ due to the axial symmetry and the spin scalar character of ρ) one gets

$$j_k(\vec{r}) = \tfrac{1}{2}\sum_{\alpha\alpha'}\mathrm{Im}(\rho_{\alpha\alpha'})[\nabla_k\varphi_\alpha(\vec{r})\varphi_{\alpha'}^*(\vec{r}) - \varphi_\alpha(\vec{r})\nabla_k\varphi_{\alpha'}^*(\vec{r})]. \tag{D15}$$

From the definition relations (D10) and (D11) one obtains

$$j_r(\zeta,\eta) = \frac{c_z c_\perp{}^3}{2\pi}e^{(\xi^2-\eta)}\sum_{\alpha\alpha'}\{\mathrm{Im}(\rho_{\alpha\alpha'})M_{n_z}M_{n_z'}N_n^\Lambda N_{n'}^{\Lambda'}\delta_{\Lambda\Lambda'}\eta^{(\Lambda-1)/2}H_{n_z}(\xi)H_{n_z'}(\xi)[\bar{L}_n^\Lambda(\eta)L_{n'}^{\Lambda'}(\eta) - L_n^\Lambda(\eta)\bar{L}_{n'}^{\Lambda'}(\eta)]\} \tag{D16}$$

and

$$j_z(\zeta,\eta) = \frac{c_z{}^2c_\perp{}^2}{2\pi}e^{(\xi^2-\eta)}\sum_{\alpha\alpha'}\{\mathrm{Im}(\rho_{\alpha\alpha'})M_{n_z}M_{n_z'}N_n^\Lambda N_{n'}^{\Lambda'}\delta_{\Lambda\Lambda'}\eta^\Lambda L_n^\Lambda(\eta)L_{n'}^\Lambda(\eta)[\bar{H}_{n_z}(\xi)H_{n_z'}(\xi) - H_{n_z}(\xi)\bar{H}_{n_z'}(\xi)]\}. \tag{D17}$$

(3) *The matrix elements.* From the preceding expressions for j_r^q and j_z^q one gets, according to Eq. (2.33), the components I_r^q and I_z^q of the fields $\vec{I}^q(\vec{r})$. Now, integrating by parts the second term of

$$\langle\alpha|W_1|\alpha'\rangle = \frac{1}{2i}\langle\alpha|\vec{I}^q\cdot\vec{\nabla} + \vec{\nabla}\cdot\vec{I}^q|\alpha'\rangle, \tag{D18}$$

the matrix element to be computed becomes

$$\langle\alpha|W_1|\alpha'\rangle = \frac{1}{2i}\int\{\varphi_\alpha^*(\vec{r})\vec{I}^q(\vec{r})\cdot\vec{\nabla}\varphi_{\alpha'}(\vec{r}) - [\vec{\nabla}\varphi_\alpha^*(\vec{r})\cdot\vec{I}^q(\vec{r})\varphi_{\alpha'}(\vec{r})\}d^3r, \tag{D19}$$

that is, with our notation,

$$\begin{aligned}\langle\alpha|W_1|\alpha'\rangle = {}& -i\delta_{\Omega\Omega'}\delta_{\Lambda\Lambda'}M_{n_z}M_{n_z'}N_n^\Lambda N_{n'}^{\Lambda'}c_\perp{}^2c_z \\ & \times\int_0^\infty e^{-\eta}\eta^\Lambda d\eta\int_{-\infty}^\infty e^{-\xi^2}d\xi \\ & \times\{c_\perp H_n(\xi)H_{n'}(\xi)I_r(\eta,\xi)\eta^{-1/2}[L_n^\Lambda(\eta)\bar{L}_{n'}^{\Lambda'}(\eta) - \bar{L}_n^\Lambda(\eta)L_{n'}^{\Lambda'}(\eta)] \\ & + c_zL_n^\Lambda(\eta)L_{n'}^{\Lambda'}(\eta)I_z(\eta,\xi)[H_n(\xi)\bar{H}_{n'}(\xi) - \bar{H}_n(\xi)H_{n'}(\xi)]\}.\end{aligned} \tag{D20}$$

*Present address: Institut Laue-Langevin, BP 156X, 38042 Grenoble-Cedex, France.
[1]M. J. Giannoni and P. Quentin, Phys. Rev. C 21, 2060 (1980).
[2]D. Vautherin and D. M. Brink, Phys. Rev. C 5, 626 (1972).
[3]D. Vautherin, Phys. Rev. C 7, 296 (1973).
[4]H. Flocard, P. Quentin, A. K. Kerman, and D. Vautherin, Nucl. Phys. A203, 433 (1973).
[5]M. Beiner, H. Flocard, Nguyen Van Giai, and P. Quentin, Nucl. Phys. A238, 29 (1975).
[6]See, e.g., P. Quentin and H. Flocard, Ann. Rev. Nucl. Part. Sci. 28, 523 (1978).
[7]Y. M. Engel, D. M. Brink, K. Goeke, S. J. Krieger, and D. Vautherin, Nucl. Phys. A249, 215 (1975).
[8]See also H. Flocard, Nukleonika 24, 19 (1979).
[9]Their $\vec{r}$ dependence has been omitted for the sake of conciseness.
[10]P. Gombás, Ann. Phys. (Leipzig) 10, 253 (1952).
[11]G. Ripka, Adv. Nucl. Phys. 1, 189 (1968).
[12]In this respect, we are indebted to P. Gara (Bureau de Calcul, IPN Orsay) for having provided us with a very efficient routine.
[13]P. Quentin and R. Babinet, Nucl. Phys. A156, 365 (1970).
[14]H. Flocard, P. H. Heenen, and D. Vautherin, in *Time-dependent Hartree-Fock Method,* edited by P. Bonche, B. Giraud, and P. Quentin (Editions de Physique, Orsay, 1979), p. 50; Nucl. Phys. (to be published).
[15]In a recent paper K. Goeke [Phys. Rev. Lett. 38, 212 (1977)] has solved the first Hamilton equation for isoscalar monopole vibrations in $\vec{r}$ representation. The comparison of his "exact" results with those obtained by perturbation techniques shows indeed a very poor convergence of the latter.
[16]H. Flocard, thèse d'Etat, Université Paris-Sud, 1975 (unpublished).
[17]J. Treiner and H. Krivine, J. Phys. G 2, 285 (1976).
[18]It is clear that for very large $|\beta_2|$ values, higher multipole moments should be included in the analysis, which has not been done here.
[19]M. J. Giannoni, F. Moreau, P. Quentin, D. Vautherin, M. Vénéroni, and D. M. Brink, Phys. Lett. B65, 305 (1976).
[20]We have used a 9 oscillator shell basis for nuclei with $A \leq 90$ and an 11 oscillator shell basis for $A > 90$.
[21]O. Bohigas, A. M. Lane, and J. Martorell, Phys. Rep. 51, 267 (1979).
[22]D. M. Brink and R. Leonardi, Nucl. Phys. A258, 285 (1976).
[23]M. Baranger and M. Véneroni, Ann. Phys. (N.Y.) 114, 123 (1978); D. M. Brink, M. J. Giannoni, and M. Véneroni, Nucl. Phys. A258, 237 (1976).
[24]F. M. H. Villars, Nucl. Phys. A285, 269 (1977).
[25]K. Goeke and P. G. Reinhard, Ann. Phys. (N.Y.) 112, 328 (1978); P. G. Reinhard and K. Goeke, Nucl. Phys. A312, 121 (1978).
[26]P. Bonche and P. Quentin, Phys. Rev. C 18, 1891 (1978). P. Bonche, H. Doubre, and P. Quentin, Phys. Lett. 82B, 5 (1979).
[27]M. J. Giannoni, D. Vautherin, M. Véneroni, and D. M. Brink, Phys. Lett. B63, 8 (1976).
[28]S. Fallieros, Lecture Notes, Orsay, 1975 (unpublished).
[29]H. Krivine, J. Treiner and O. Bohigas, Nucl. Phys. (to be published); J. Treiner and H. Krivine, in *Time-dependent Hartree-Fock Method,* edited by P. Bonche, B. Giraud, and P. Quentin (Editions de Physique, Orsay, 1979), p. 194.
[30]Since $U_2 = P_0\, e^{i\frac{\pi}{2}} i\sigma_2$, the U_2 transformation amounts for the space variables only to a change of (r, z, θ) into $(r, z, -\theta)$.
[31]The Bateman Manuscript Project, *Higher Transcendental Functions,* edited by A. Erdelyi (McGraw-Hill, New York, 1953), Vol. II.